ELSEVIER

Journal of Hydrology 173 (1995) 263–282

Journal of Hydrology

Stagnant aquifer concept Part 3. Stagnant miniaquifers in the stage of formation, Makhtesh Ramon, Israel

Vladimir Fridman[a], Emanuel Mazor[a,b,*], Alexander Becker[b], Dudik Avraham[c], Eilon Adar[c]

[a]*Department of Environmental Sciences and Energy Research, Weizmann Institute of Science, Rehovot 76100, Israel*

[b]*Ramon Science Center, J. Blaustein Institute of Desert Research, Ben-Gurion University of the Negev, Mitzpe Ramon 80600, Israel*

[c]*Department of Water Resources, J. Blaustein Desert Research Institute, Ben-Gurion University of the Negev, Sde Boqer Campus 84990, Israel*

Received 21 June 1994; revision accepted 29 January 1995

Abstract

Observation wells in the arid Ramon National Geological Park were monitored at three sites (C, T, and E), each with wells spaced tens of meters apart, the distances between the sites being 860–1060 m. The following characteristics were observed: (1) water level differences of up to a few meters occur between wells that are 20–60 m apart at each site, and level differences of over 10 m occur between wells at the three sites, (2) the water levels were steady over 2 years of monitoring, (3) Cl concentrations in the wells vary over three orders of magnitude: 0.4–1.8 g l^{-1} in site C, 1.8–3.7 g l^{-1} in site T, and 2.5–13 g l^{-1} in site E, (4) the relative abundance patterns of the dissolved ions vary remarkably along with the concentration variations, from water dominated by Ca and SO_4 to water dominated by Na and Cl, (5) the chemical composition is steady in each well, as indicated by chemical analyses repeated over 6 years, and conductivity monitoring over 2 years. The observed significant and steady compositional differences are interpreted as indicating the existence of small-scale isolated aquifers, with no lateral flow between them in spite of the pronounced water level differences. Flow in fractures is ruled out because of the steady water levels and very slow water level recovery in pumped wells.

Dating strongly confirmed the lack of flow in the investigated shallow system. A well situated in the flood plain of Nahal Ramon revealed a tritium concentration of 8 TU and ^{14}C concentration of 69 p.m.c. — indicating post-1954 water, but two wells outside the river bed contained no measurable tritium and ^{14}C values of 14 and 22 p.m.c. — indicating water ages in the order of 10 000 years. In 15 additional wells no measurable tritium was determined. Thus, a

* Corresponding author.

0022-1694/95/$09.50 © 1995 – Elsevier Science B.V. All rights reserved
SSDI 0022-1694(95)02708-4

case of ancient groundwater trapped in shallow aquifers, and bounded by efficient hydraulic barriers, is demonstrated.

The geological set up seemed rather homogeneous, with no clue to small-scale efficient hydrological barriers. Yet, a detailed geological study, conveyed in the light of the hydrochemical findings, revealed the existence of dykes and small-scale structural and lithological controls, coinciding with some of the hydraulic discontinuities defined by the water properties.

1. Introduction

Hydraulic continuity is often assumed for groundwater systems situated in what seems to be uniform geological units, and hydraulic interconnections are often assumed even for systems observed to be hydraulically heterogeneous. However, research connected to pollution and tracer applications is producing a growing body of evidence for the occasional existence of small-scale hydraulic discontinuities. A major problem in studies of this nature is that they are conducted after a system is found to be contaminated, and thus base data for the non-disturbed system are lacking. The present study concerns an uncontaminated region.

A unique opportunity to study shallow (around 20 m deep) trapped groundwaters, separated by small-scale hydraulic discontinuities, came up in the eastern part of the Ramon National Geological Park, located in the arid southern part of Israel (Fig. 1(a)). Abundant closely spaced prospecting boreholes were observed to contain water at different levels, a few years after their dry completion. The geology seemed simple, providing no clue of hydraulic discontinuities or entrapment of old groundwater. The decision to undertake a detailed study was based on the following advantages (1) the area is still virgin hydrologically, i.e. no water has been abstracted and no sewage has been released in this region, (2) the ongoing mining activity promised a wealth of detailed geological information. The groundwater system was monitored for water level, chemical analyses and in situ electric conductivity measurements, and a detailed geological study and some water dating were conducted.

2. Results — the 1000 m scale

The study area is located near the dry river bed of Nahal Ramon, in the eastern part of the Makhtesh Ramon (Fig. 1(a)). The overall geological picture (Fig. 1(b)) is given by Bentor and Vroman (1951), Zak (1968), Bartov et al. (1972), Hirsh (1980), Garfunkel (1987) and Kohn et al. (1988). Eighteen abandoned prospecting boreholes were used as observation wells in the present study (Fig. 1(c)). The wells, 18–27 m deep, and with 3–8 m of groundwater, are grouped in sites C, T and E (Fig. 1(d)), the distance between C and T being 1060 m and between T and E 860 m.

The water level was monitored over 2 years, with an instrumental error of ± 2 cm. A detailed geodetic survey was conducted in order to express the water levels in altitude values of m.a.s.l. (meters above sea-level), the measuring error being ± 0.5 cm. A very

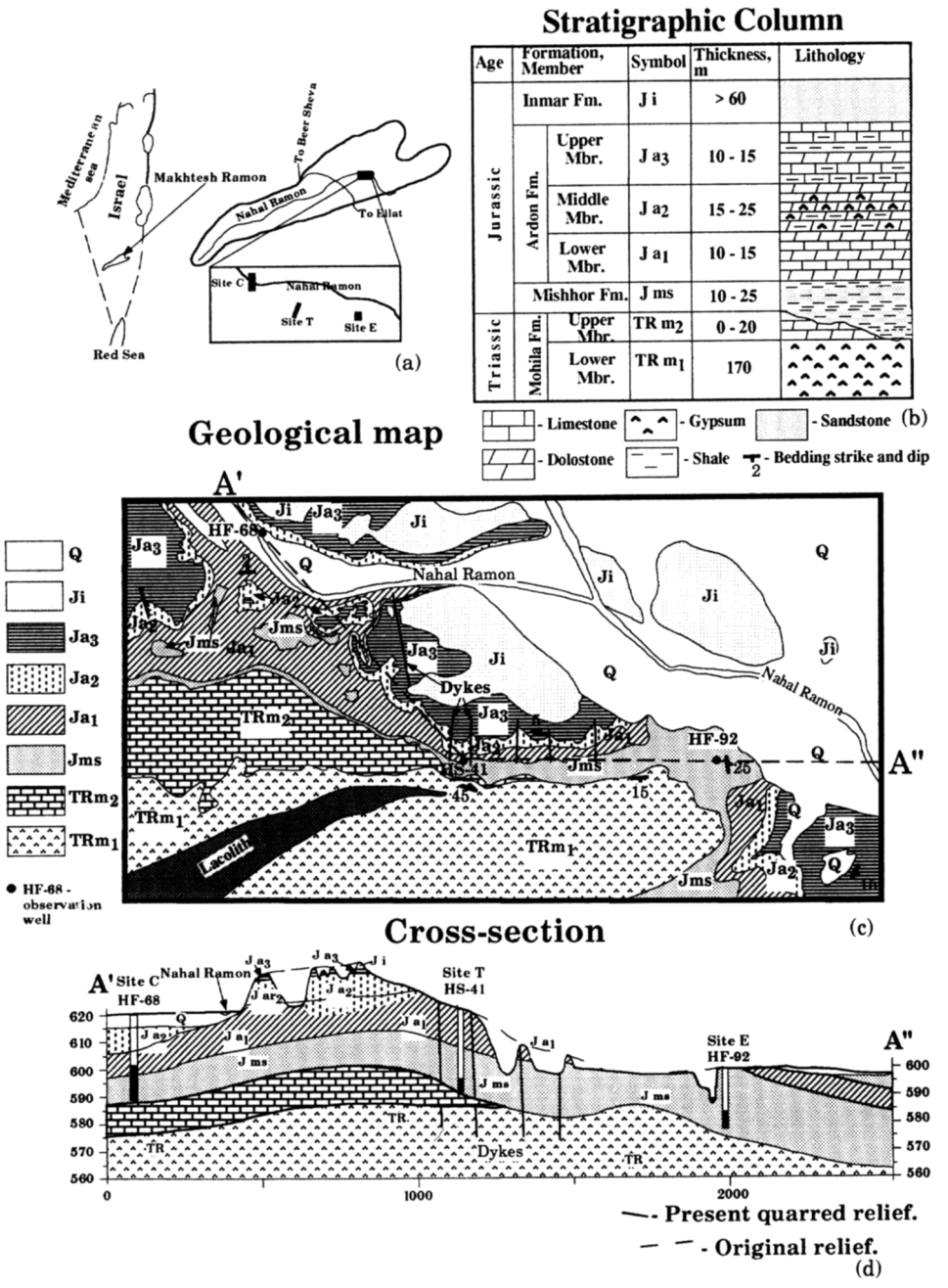

Fig. 1. (a) Study area and location of sites C, T and E; (b) stratigraphic column (adapted from Buchbinder and Le Roux, 1993); (c) geological map; (d) cross-section (with one representative well entered for each site).

special pattern emerged (Fig. 2): (1) steady water levels in each well, with no seasonal fluctuations, (2) pronounced differences between the water levels at the three sites, and smaller but significant differences between adjacent wells within each site, (3) the water level differences were maintained over 2 years of monitoring.

The average water table at site C is 5 m higher than the average level at site T, and the average level at site T is 12 m higher than the average level at site E. A basic research question is whether one deals with an 'active hydraulic gradient', i.e. whether groundwater flows from C to T and E? Or, whether one deals with a 'false hydraulic gradient', as sites C, T and E are hydraulically disconnected?

Electrical conductivity was monitored with an instrumental error of ±0.5% of the measuring value, revealing the following pattern (Table 1 and Fig. 2): (1) the electrical conductivity is low at site C, intermediate at site T and highest at site E, the total range being large, from 0.8 to 30.9 mS cm^{-1}, equivalent to a TDI range of 13–800 mequiv. l^{-1}, (2) distinct conductivity values were observed also between adjacent wells at each

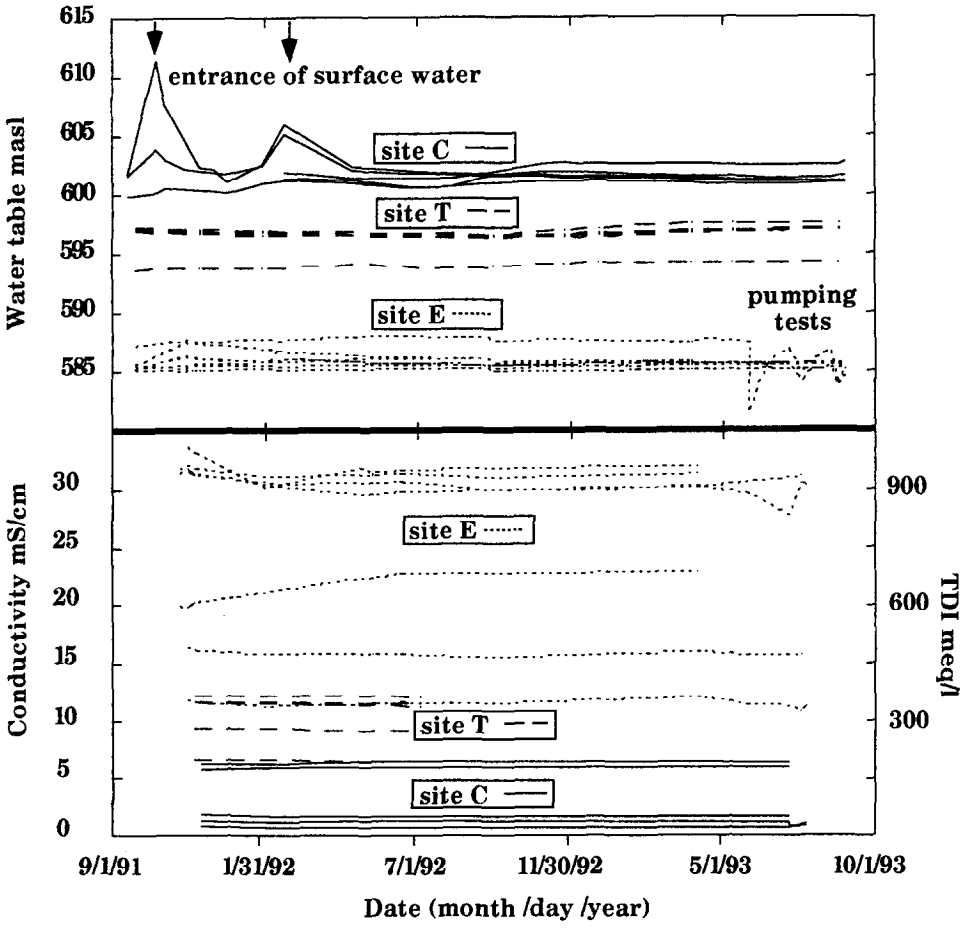

Fig. 2. Water level and electric conductivity time series, all wells.

Table 1
Field and laboratory data

Well	Date	Hydr. head m.a.s.l.	Samp.	Cond.	T	K	Mg	Ca	Na	Cl	SO_4	HCO_3	NO_3	TDI	Trit.	±	^{13}C	^{14}C	±
Site C																			
HF-64	30.12.92	601.2	s	0.6	23.5	3.7	28	55	44	54	136	130	15.0	467	0	0.4			
HF-68	30.12.92	601.2	s	0.7	24.0	4.4	37	95	45	57	155	277	6.0	677	8.9	0.3			
HF-68	14.07.93	601.2	p			3.6	30	70	36	50	118	204	4.0	515	9.7	0.4	−7.8	68.7	0.5
HF-26	30.12.92	600.9	s	1.6	24.1	4.2	52	123	243	313	330	252	24.0	1341					
ES-1	30.12.92	602.5	s	6.2	24.3	9.8	141	383	1090	1870	1000	202	100.0	4795	0.4	0.3			
HF-33	30.12.92	601.4	s	5.9	24.1	8.6	151	428	1000	1530	1300	190	58.0	4666	1.6	0.3			
Site T																			
HS-41	23.12.92	594.2	s	6.6	24.3	10.0	161	562	897	1363	1800	200		4993	3	0.3			
YT-6	23.12.92	597.0	s	12.2	24.1	21.3	400	1112	1323	3681	1855	111		8503	0.3	0.2			
YT-2	23.12.92	597.1	s	11.7	24.0	21.3	389	1031	1294	3420	1850	143		8148	0	0.2			
YT-3	23.12.92	596.9	s	11.6	24.1	20.8	384	1011	1294	3386	1850	163		8109	0	0.3			
YT-4	23.12.92	597.0	s	11.6	24.1	19.2	320	971	1441	3345	1800	141		8037	0	0.2			
HS-40	23.12.92	597.6	s	9.2	24.2	14.3	220	702	1323	2035	2250	148		6692					
Site E																			
YT-13	9.09.92	585.7	s	22.5	23.6	46.5	806	1226	3550	7896	2700	190		16415	1.7	0.2			
YT-8	9.09.92	585.2	s	31.5	23.7	53.0	1476	1906	4320	12825	2550	228		23358	0.1	0.2			
YT-7	9.09.92	585.9	s	31.0	24.1	56.0	1428	1984	4165	12445	2400	176		22653	1.1	0.3			
DU-2	9.09.92	585.5	s	29.3	23.8	56.0	1339	1740	4165	11815	2550	220		21885	0.7	0.3			
HF-92	9.09.92	585.5	s	17.9	23.6	50.0	798	1302	2450	6709	2500	131		13940	1.8	0.3			
HF-92	16.08.93	585.4	p	34.0	24.1	47.2	1517	1889	3850	12166	2050	111	30.0	21661	0.7	0.2	−7.8	13.6	0.2
YT-12	9.09.92	587.6	s	11.4	24.0	34.0	351	759	1760	3038	2100	132		8174	1.1	0.3			
YT-12	16.08.93	587.7	p	10.6	24.3	33.0	323	721	1400	2534	2000	172	9.0	7192	0.7	0.3	−12	22.4	0.4
YT-11	9.09.92	585.7	s	15.4	24.4	46.5	535	1156	2000	5230	2350	126		11444	0	0.2			
Pond E	9.09.92		s	144.0	30.9	200.0	8730	5887	40000	74322	3800	179		133118	6.9	0.3			
Pond E	9.07.93		s			330.0	10915	6258	48000	113400	2400	161	576.0	182040					

Column Samp: s, sample collected with sampler; p, sample collected during pumping. Major ions (mg l^{-1}) conductivity (mS cm^{-1}), temperature (°C), ^{13}C, (‰), tritium (TU), ^{14}C (p.m.c.)

site, (3) the electrical conductivity was steady in each well over 2 years of monitoring, reflecting steady salinity values.

The chemical composition was analyzed in samples collected four times in the period 1986–1992 (Fridman, 1994), and the reproducibility for Na, Ca, Mg and Cl was high (±10% or better, Fig. 3), revealing: (1) high analytical quality, and (2) the composition remained steady — in good agreement with the steady values observed during the electrical conductivity monitoring. In contrast, the reproducibility of the SO_4 and HCO_3 measurements was poor (Fig. 3). In view of the steady values of the conductivity in each well it seems that the behavior of the latter ions indicates analytical problems (including possible bacterial processes in some of the sampling bottles), rather than natural fluctuations. This conclusion is supported by the high reproducibility of the Na, Mg, Ca and Cl data. Thus, the SO_4 and HCO_3 data are taken as orders of magnitude only.

The dissolved ion concentrations at site C are considerably lower than the concentrations at sites T and E, as revealed in the range diagrams of Cl and SO_4 (Fig. 4, logarithmic scale!). Measuring conductivity alone, or merely Cl concentration, one could conclude that sites T and E host similar waters. Yet, the finger print diagrams (Fig. 4) reveal significant compositional differences.

The composition diagrams of Na, Ca and Mg as a function of Cl (Fig. 5) reveal two lines: line I of the fresher water of C and some of the wells of site T, and line II which is composed of the rest of the wells of site T and all the wells of site E. Thus, different

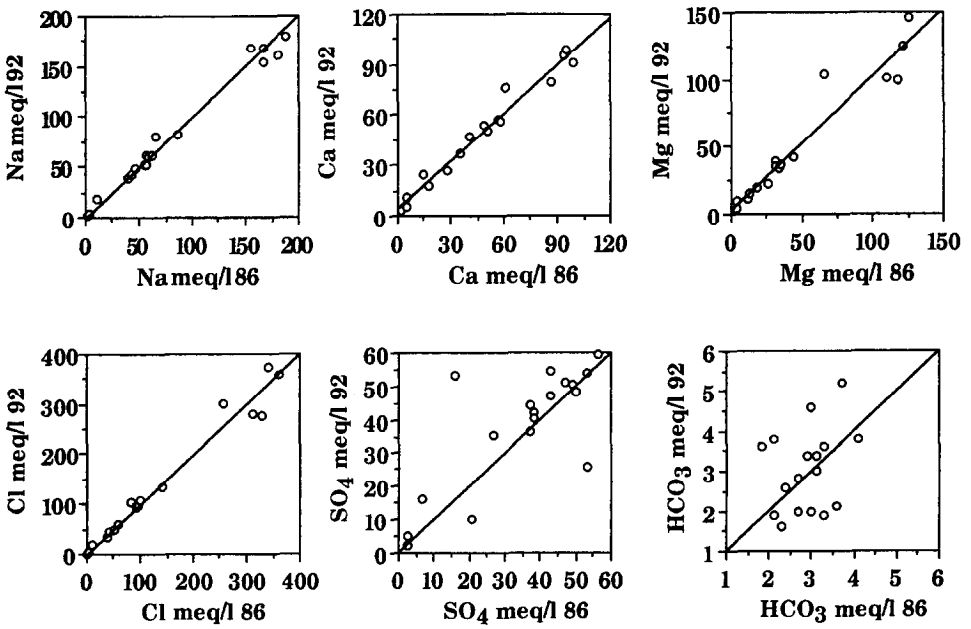

Fig. 3. Reproducibility check: repeated chemical analyses undertaken during 1986 and 1992 (Fridman, 1994). The reproducibility is seen to be high for Na, Ca, Mg and Cl. This reveals also that the composition remained steady in each well.

hydrochemical evolution paths are recognizable, further demonstrating the enormous heterogeneity of the groundwater system in the region studied. This topic is discussed later in the paper.

Seventeen wells were analyzed for tritium and three wells were analyzed for ^{14}C. Only well HF-68, located on the flood plain of Nahal Ramon, revealed postbomb values of 8 TU (direct entrance of runoff seems likely). The rest of the wells revealed no measurable tritium (Table 1), indicating a water age that is greater than 35 years. Limited ^{14}C data from site E indicated water ages in the order of 10^4 years (discussed in a later section).

The local geology seemed homogeneous at the initial stage of the study, and no

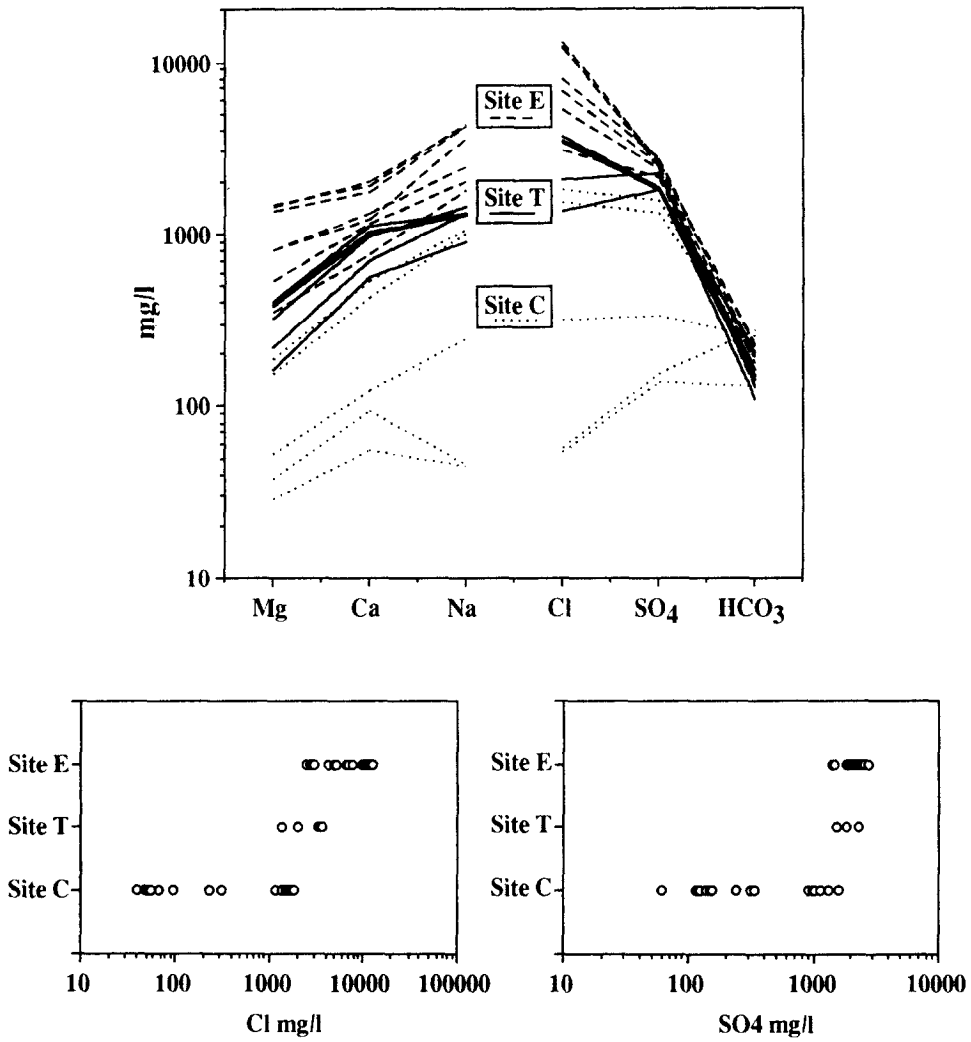

Fig. 4. Finger print diagrams and range diagrams, all wells.

hydrological barriers were anticipated. However, a detailed geological study, which followed the hydrochemical monitoring, revealed geological controls that fit the observed hydrochemical heterogeneity and the multitude of separate, yet steady, water levels. The wells of site C tap their fresh water in sandstone interbeds of the Mishhor Formation, whereas the saline waters of the wells at sites T and E occur in sandy shale of the Mishhor Formation (Fig. 1(d)). In addition, the three sites are separated by kaolinized dykes, 1–5 m thick (Figs. 1(c) and (d)), that were not seen on the surface but were revealed in the mining excavations.

Flow in fractures is ruled out for the three sites for the following reasons: (1) the water levels and composition of dissolved ions are remarkably steady in the individual wells; (2) tritium was found to be on the limit of detection indicating an effective water age of more than 35 years; (3) recovery in the wells after pumping was very slow (several months); (4) the fracture distribution in the area was studied in detail, three types of fractures were found — two systematic sets of joints (of the type described by

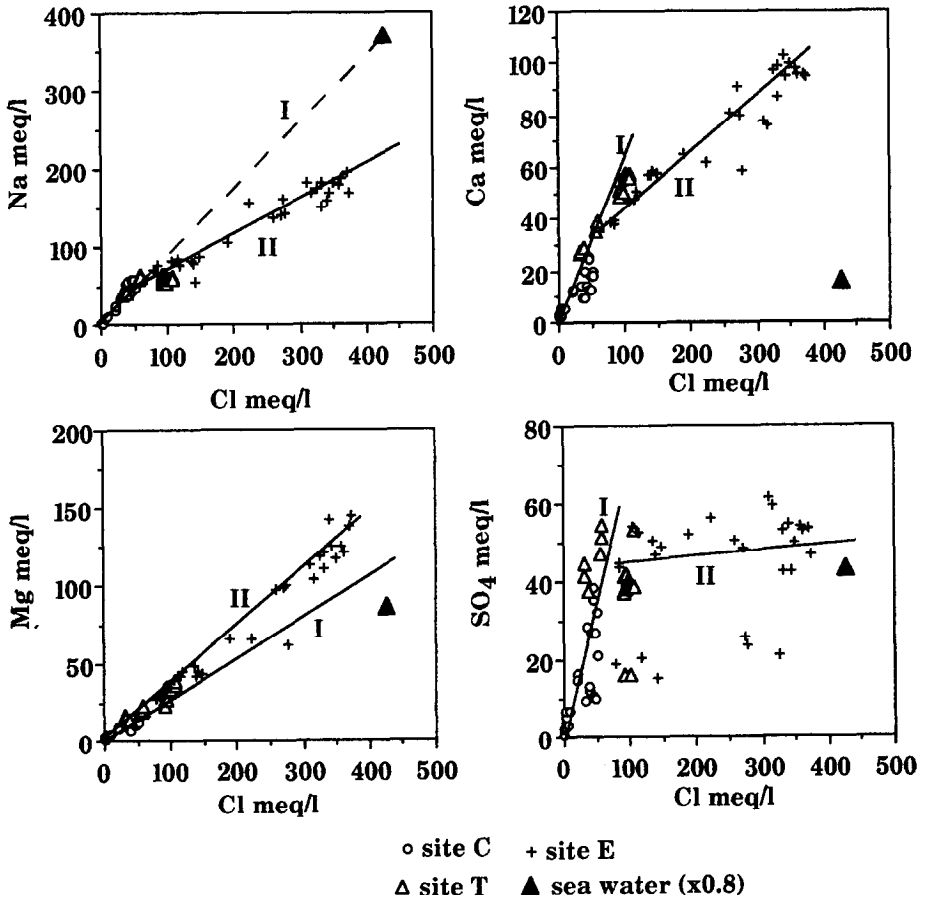

Fig. 5. Composition diagrams, years 1986–1993 (table 1, Fridman, 1994). Lines I and II are discussed in the text.

Hobbs (1967) and Gross (1993a)), and non-systematic fractures and faults (of the type described by Hodgson (1961), Hachock (1985), and Gross (1993b)). Fractures in the area studied occur in the relatively competent layers of limestone, dolostone, sandstone and siltstone, and are absent in the shale and clay interbeds. The latter are widely distributed in the section and constitute mechanical barriers for flow in fractures.

In summary, sites C, T and E constitute three isolated groundwater systems, observable at the 1000 m scale. The systems could be identified only by different properties which were revealed by monitoring of water levels and electrical conductivity, detailed chemical analyses, groundwater dating, and a detailed geological study.

Groundwater is seen to occur in the study area in hydraulically isolated rock bodies, not only at the discussed 1000 m scale, but as shown in the following sections also at the 20 m scale. Thus, the isolated groundwater systems described are intermediate between the miniscale of fluid inclusions and the large-scale of stagnant (trapped), commonly pressurized, aquifers which can sustain water-supply wells. Hence. the term miniaquifer in suggested for the observed stagnant water systems.

3. Results — the 20 m scale

3.1. Site C

Five wells, spread along a strip of 800 × 150 m, were monitored in site C (Fig. 6(a)). The wells are drilled in sandstone of the Mishhor Formation (Figs. 1(a) and (d)), and no geological discontinuities were observable.

Well HF-68 was pumped for 2 h at a rate of 1 l min^{-1}, and a drawdown of 1.5 m was observed, which fully recovered after 4 h. Applying single borehole methods, a hydraulic conductivity of 5×10^{-6} m s^{-1} has been calculated, in the range expected for sands or sandstones.

The following patterns were observed for the wells of site C (Fig. 6): (1) small but distinct differences of hydraulic head and electrical conductivity between the wells, (2) these features were remarkably steady, and the differences between the wells were maintained over the 2 years of study.

The finger print diagram seen in Fig. 7 reveals three hydrochemical groups: (1) CI (wells HF-64 and 68) with a composition (by weight) of $Ca > Na > Mg$; $SO_4 > HCO_3 > Cl$, and 0.5 g l^{-1} TDI, (2) CII (well HF-26) with a composition of $Na > Ca > Mg$; $SO_4 > Cl > HCO_3$ and 1.3 g l^{-1} TDI, and (3) CIII (wells HF-33 and ES-1) with a composition of $Na > Ca > Mg$; $Cl > SO_4 > HCO_3$, and 6 g l^{-1} TDI.

A pumped sample from well HF-68 revealed a postbomb tritium concentration (8 TU), and a rather high ^{14}C concentration (68.7 p.m.c.), possibly reflecting a direct inflow of flood water into the well.

In summary, two inferred hydraulic discontinuities are marked on the transect given in Fig. 8, separating three miniaquifers: (1) a miniaquifer bordering the flood plain of Nahal Ramon, possibly recharged by the river, as revealed by its fresh (type

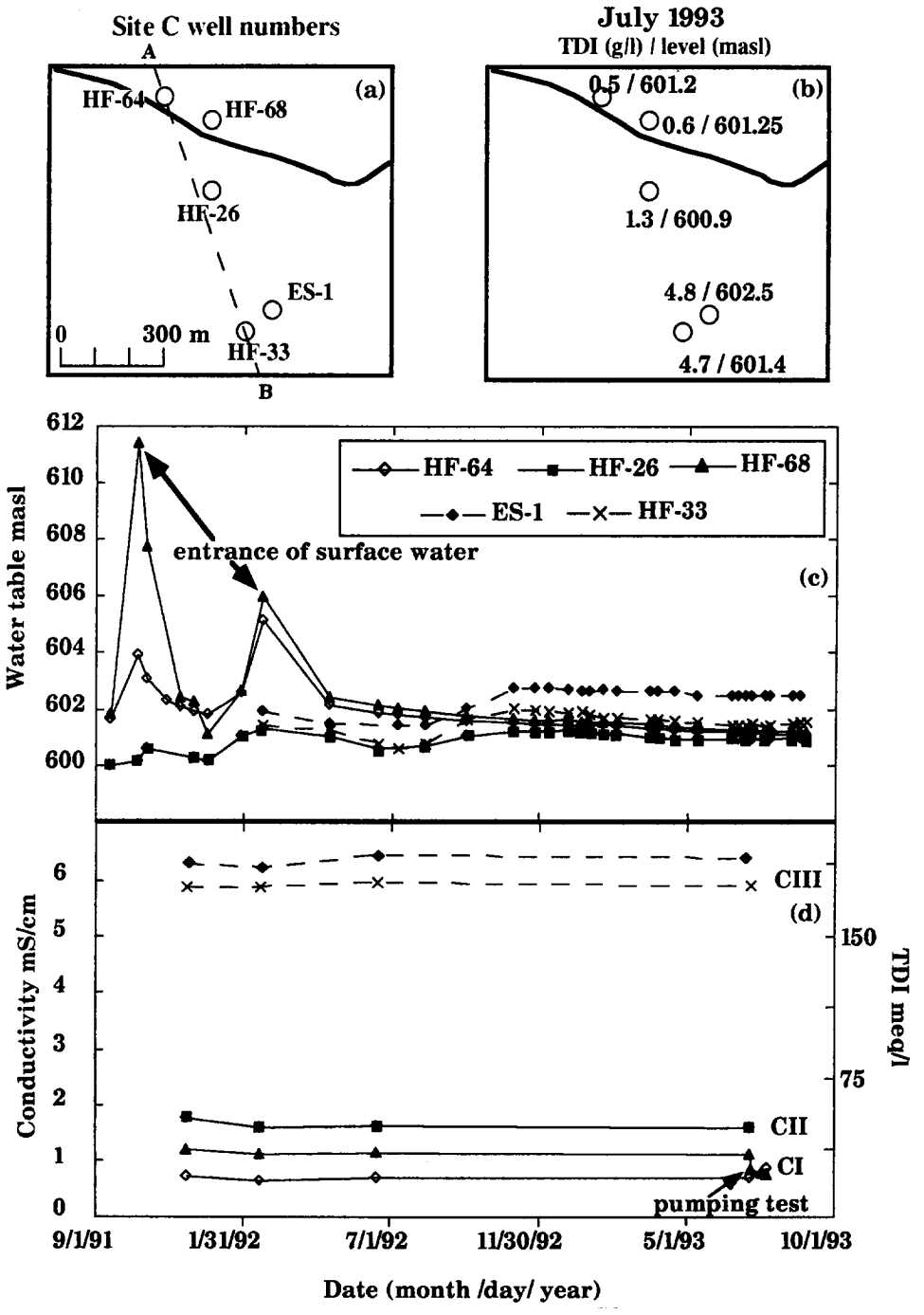

Fig. 6. Site C: (a) well location; (b) TDI and water level map; (c) water level time series; (d) electrical conductivity time series.

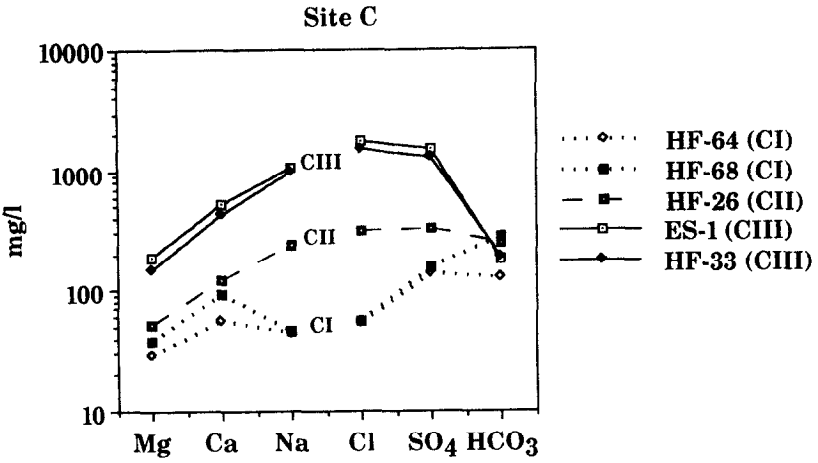

Fig. 7. Site C: finger print diagram. Groups CI, CII and CIII are discussed in the text.

CI) water, (2) a miniaquifer with type CII water, that is distinct owing to its salinity and composition, and (3) a miniaquifer with a water table that is 0.7 m higher than that in the adjacent wells, and contains type CIII water, which is old as it contains no measurable tritium. So far no potential geological barriers have been identified at site C. This outcome demonstrates that geological information alone can not reveal the nature of groundwater flow, nor delineate hydraulic interconnections or discontinuities. To do so the properties of the water itself have to be thoroughly studied.

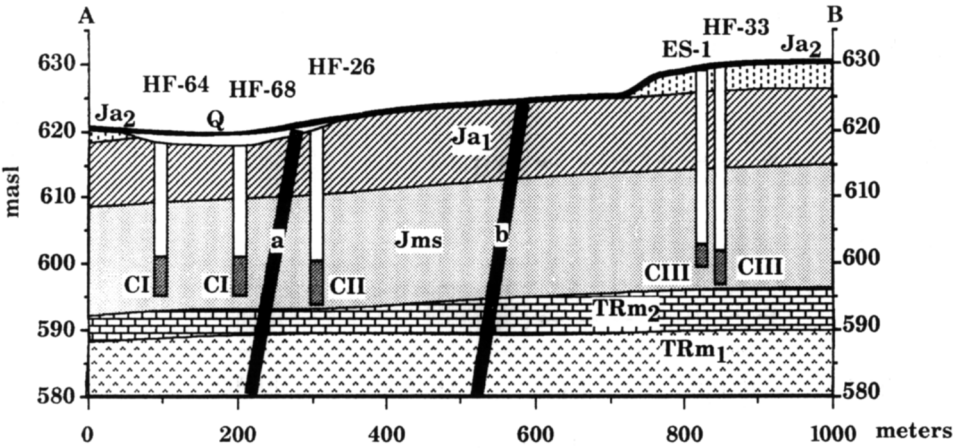

Fig. 8. Site C: transect A–B (Fig. 6(a)). Water levels are marked for each well (shading). Inferred hydraulic discontinuities 'a' and 'b' (black lines) and miniaquifers hosting water groups CI, CII and CIII are discussed in the text.

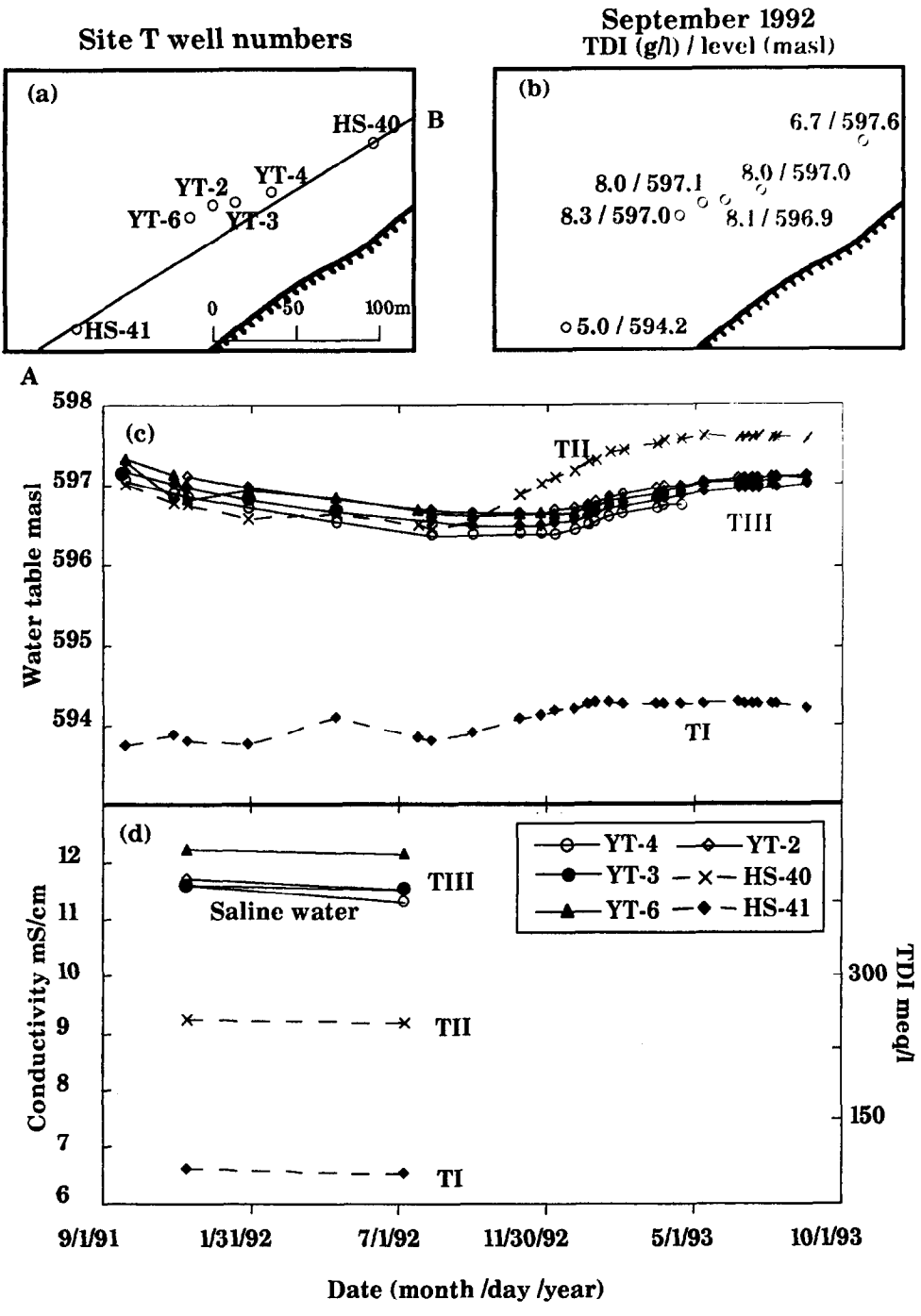

Fig. 9. Site T: (a) well location; (b) TDI and water level map; (c) water level time series; (d) electrical conductivity time series.

3.2. Site T

Six observation wells are spread along a 200 × 30 m strip, about 600 m away from the Nahal Ramon dry bed (Fig. 9(a)). The wells are drilled into sandy shale interbeds of the Mishhor Formation, the site being crossed by a number of north–south kaolinized dykes (Figs. 1(c) and (d)), 1–5 m wide.

The hydrographs seen in Fig. 9(c) reveal (1) two major water levels — a low one seen in well HS-41, and one 3 m higher seen in the rest of the wells which are only 120 m away, (2) this level difference was steady over the monitoring period, and (3) the detailed behavior of the hydrographs reveals that well HS-40 had a slightly different pattern than that of wells YT-6, 2, 3, and 4. Repeated electrical conductivity measurements (Fig. 9(d)) revealed distinct differences in salinity that were maintained in repeated measurements.

Combining the salinity data, hydraulic heads, and the geographical distribution of the wells, three miniaquifers emerge: TI — represented by the fresh water well HS-41; TII — medium salinity water, of well HS-40, with a water level 3 m higher than TI; and TIII — relatively saline water, including wells YT-6, 2, 3 and 4, with a water table similar to that of TII.

The finger print diagram of Fig. 10 and Table 1 reveal that the three groups of site T differ in their relative ionic abundances, as well as the total salinities. Two wells HS-40 and HS-41 contain groundwater with composition (by weight) $Na > Ca > Mg$; $SO_4 > Cl > HCO_3$ and 5–7 g l^{-1} TDI. Wells YT-2, 3, 4 and 6 contain groundwater with a composition of $Na \approx Ca > Mg$; $Cl > SO_4 \gg HCO_3$ and 8 g l^{-1} TDI.

In summary, two hydraulic discontinuities are observed at site T (Fig. 11), separating the three miniaquifers TI, TII and TIII. The hydraulic discontinuity 'a' between TI and TII coincides with an observed kaolinized dyke, one of a number of dykes observed in the area of site T (Figs. 1(c) and (d)). No geological control was identified for the second discontinuity 'b'.

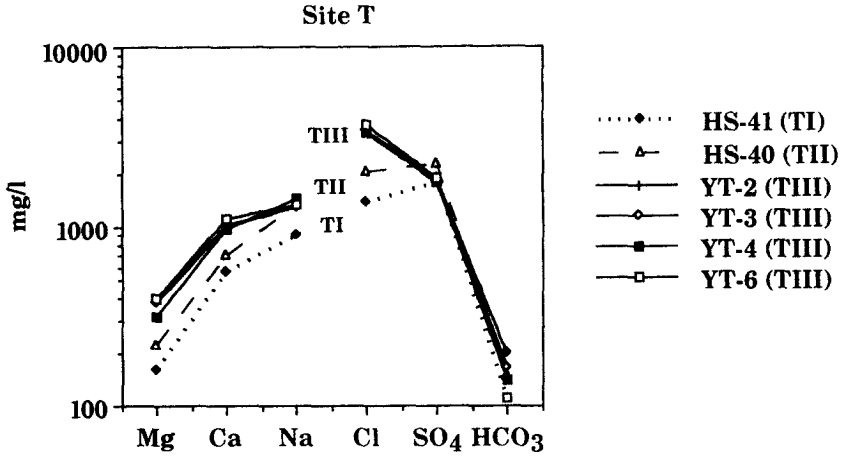

Fig. 10. Site T: finger print diagram.

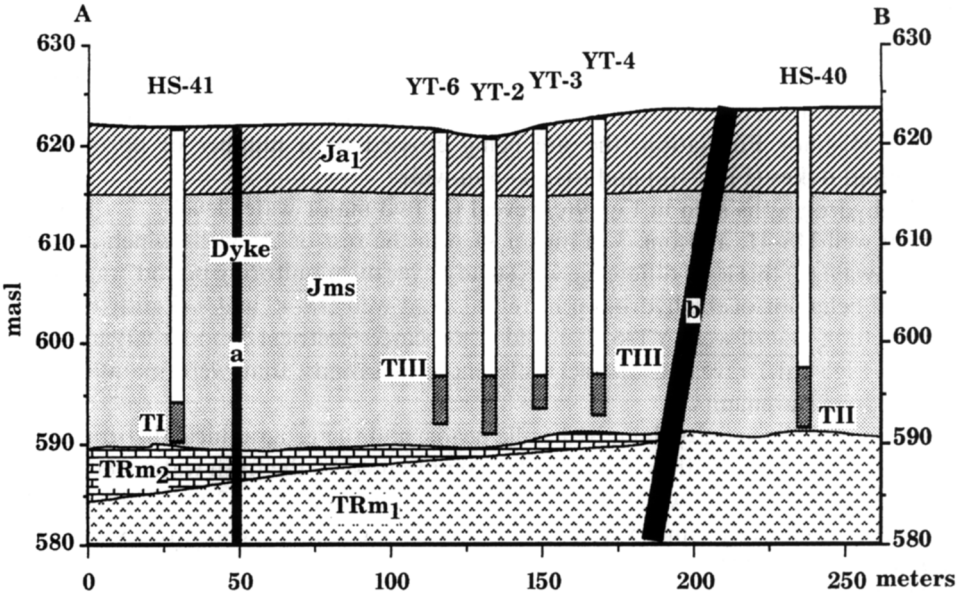

Fig. 11. Site T: transect A–B (Fig. 9(a)). Water levels are marked for each well (shading). Inferred hydraulic discontinuities 'a' and 'b' (black lines) and miniaquifers hosting water groups TI, TII and TIII are discussed in the text.

3.3. Site E

Seven observation wells are located along a 80 × 30 m strip, 400 m from the Nahal Ramon dry river bed (Fig. 12(a)). The wells are drilled into the sandy shale of the Mishhor Formation (Figs. 1(c) and (d)).

A pronounced diversity in the salinity and hydraulic heads is observed between the closely spaced wells (Fig. 12(b)).

The hydrographs (Fig. 12(c)) reveal a hydraulic diversity: (1) the water level in well YT-12 is 2 m higher than in the other wells, including well YT-11 which is 20 m distant, and this level difference was maintained during the 2 years of monitoring, (2) well YT-13 stands out as the only well that responded to a rain event.

Well YT-12 was pumped at a rate of 3 l min^{-1} and in 10 min the level dropped 6.5 m (emptying the well), and recovery lasted over 2 months. A second pumping of this well revealed similar results. A hydraulic conductivity of only 3×10^{-8} m s^{-1} has been calculated, which is in the range observed for sandstones. Similarly, the pumping tests of well HF-92 revealed a hydraulic conductivity of 5×10^{-8} m s^{-1}.

The electrical conductivity monitoring revealed a large range of water salinities in the wells of site E, that were maintained during the monitoring period (Fig. 12(d)). Wells YT-7, YT-8, DU-2 and HF-92 are saline, wells YT-11 and YT-12 are fresh, and well YT-13 is intermediate — possibly reflecting a hydraulic pulse, induced by the mentioned rain event. The finger print diagram (Fig. 13) reveals a general similarity in

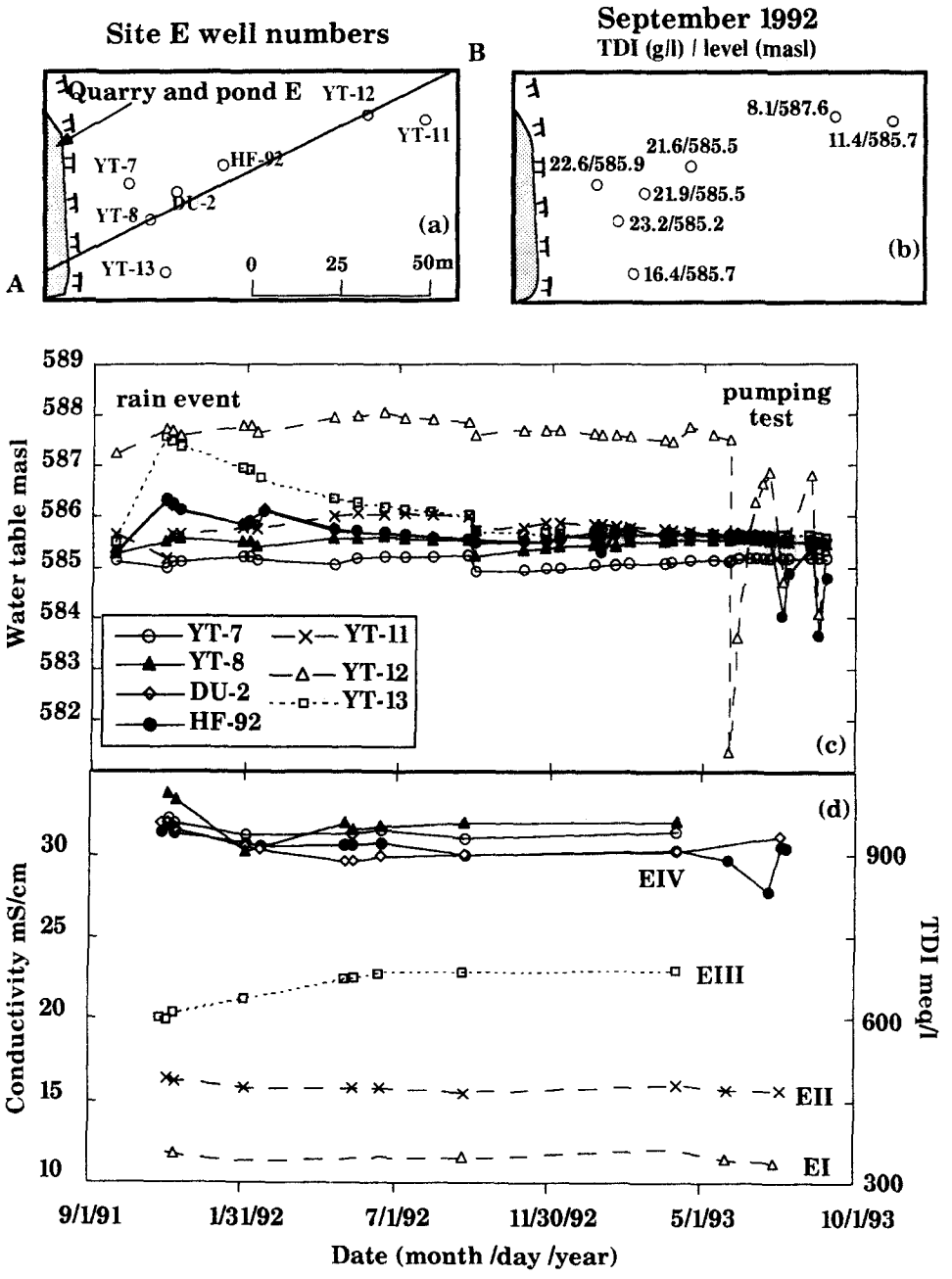

Fig. 12. Site E: (a) well location; (b) TDI and water level map; (c) water level time series; and (d) electrical conductivity time series.

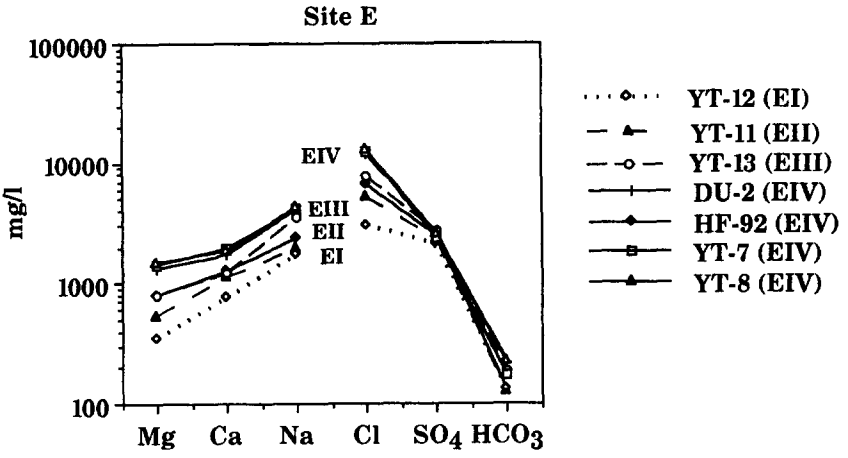

Fig. 13. Site E: finger print diagram.

the relative ionic abundances, which are (by weight): Na > Ca > Mg; Cl > SO_4 > HCO_3, but the salinity varies from 8 to 23 g l^{-1} TDI.

The wells of site E contained no measurable tritium (Table 1). Well HF-92 revealed 13.6 ± 0.2 p.m.c., along with a $\delta^{13}C$ value of −7.8‰, whereas the only 40 m distant well YT-12 revealed 22.4 ± 0.4 p.m.c., and $\delta^{13}C$ of −12‰. The ^{14}C age of the water found in well HF-92 may be estimated as follows: the $\delta^{13}C$ value of −7.8‰ seems to indicate water–carbonate rock interaction and, hence, an initial ^{14}C concentration of 60 p.m.c. may be assumed (Kroitoru et al., 1989), leading to a water age of the order of 12 000 years. The distinctly lower $\delta^{13}C$ value of −12‰, observed in the water of well YT-12, seems to indicate: (1) different paleo-vegetation and, hence, isotopically lighter soil–CO_2 or (2) water–rock interaction was less with carbonates and more with silicates, in which case the chemical decrease of the initial ^{14}C concentration was less prominent than in the case of the water in well HF-92. Accordingly, the initial ^{14}C in the well YT-12 water could have been more than 60 p.m.c., e.g. 75 p.m.c., and the age derived from the observed 22.4 p.m.c. may be around 10 000 years. The measured ^{14}C concentrations are regarded as analytically significant, but the calculated ^{14}C water ages are semiquantitative as a result of the assumptions connected to the initial ^{14}C concentrations. The main conclusions of the dating are: (1) these wells tap ancient groundwaters that differ from each other by the composition of their stable and radioactive carbon isotopes, indicating (2) water recharge in different paleo-regimes, and (3) lack of hydraulic interconnection for about 10 000 years.

In summary, four water bodies, EI–EIV, are distinguishable at site E, separated by four hydraulic discontinuities (Fig. 14): (1) separating the only 20 m distant wells YT-11 and YT-12, distinguished by different water levels and slightly but consistent differences in salinity; (2) separating well YT-12 from wells HF-92, DU-2, YT-8 and YT-7, differing by water level, salinity, and distinguished by high ^{14}C ages; (3) separating well YT-13 from the rest, as this well is the only one that responded to the flood; (4) separating the wells from the pond in the adjacent quarry, containing seeped

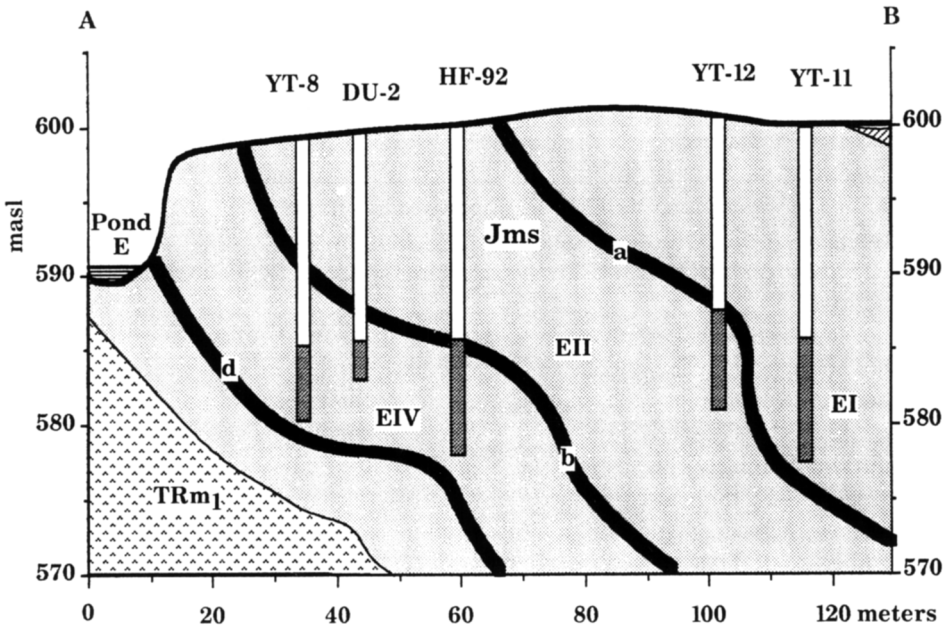

Fig. 14. Site E: transect A–B (Fig. 12(a)). Water levels are marked for each well (shading). Inferred hydraulic discontinuities a–d (black lines) and miniaquifers hosting water groups EI–EIV are discussed in the text. Wells YT-7 and YT-13 and hydraulic discontinuity 'c' are outside the transect.

water (Fig. 14). The water in the pond stood there since 1991 and was evaporated up to a total salinity of 182 g l^{-1}, and attained a composition entirely different from the water in the wells. The water level of the pond was 2 m higher than the level in the wells and had a high density, yet no contribution was noticed in the wells, including the only 20 m distant fresh water well YT-13.

No clear cut geological controls that may explain the nature of the inferred hydraulic discontinuities could be observed. However, the rock strata of the Mishhor Formation at site E are tilted to the west at an angle of 15–25°, and include facial and folding-induced lens-like structures of permeable rocks engulfed by impermeable rocks. The folding is due to bedding-plain slip, which is common in the Ramon (Becker, 1994). This is in contrast to a simple, nearly horizontal structure at sites C and T. Thus, the inferred hydraulic discontinuities may be controlled by inclined bedding and lens structures involving alternations of permeable and impermeable rocks at the 10–20 m scale.

4. Sources of the dissolved ions

Two lines are observed in the composition diagrams of Fig. 5: line I, including the fresher water of site C and some of the wells of site T, and line II which includes the rest of the wells of site T and all the wells of site E. Line I reveals a Na–Cl ratio as in

seawater, and extrapolates to the zero value. A marine airborne (atmospheric) origin for these two ions seems most plausible (the concentration variations being caused by different evapotranspiration intensities operating prior to water infiltration into the local saturated zone). Line I in the Ca–Cl plot reveals a significant Ca enrichment, as compared with the marine value, and line I in the SO_4–Cl plot reveals a similar enrichment of SO_4, suggesting dissolution of varying amounts of gypsum. Line I in the Mg–Cl plot reveals a small Mg addition over the marine airborne ratio, which can be explained by dissolution of some $MgSO_4$, commonly accompanying gypsum (the concentration of HCO_3 is too low to explain the Ca enrichment by water–calcite interaction).

Line II in the SO_4–Cl graph of Fig. 5 is almost horizontal, reflecting saturation with regards to gypsum. The highest SO_4 concentrations seen on line II are around 70 mequiv. l^{-1}, whereas the highest Ca concentrations along line II reach 100 mequiv. l^{-1}. Thus, some Ca is in excess over that expected from gypsum dissolution. Similarly, line II on the Mg–Cl plot reveals an enrichment over the atmospheric Mg that accompanied the Cl. In contrast, line II in the Na–Cl plot indicates a distinct depletion of the original marine Na, brought in with the atmospheric Cl. Thus, an ion exchange process is evident, taking Na out of the water and introducing Ca and Mg. Such an ion exchange has been observed elsewhere (Mazor, 1968; Mazor and Mero, 1969; Mazor et al., 1973, 1981).

The linear correlation demonstrated by line I of the composition plots of Fig. 5 indicates different degrees of evapotranspiration prior to infiltration into the local saturated zone. In contrast, the linear correlation reflected by line II in Fig. 5 indicates that mixing of fresh water with saline water also takes place, besides the gypsum dissolution and ion exchange.

Each of the isolated groundwater systems, observed in the present study area, hosts different combinations of the hydrochemical processes discussed.

5. Conclusions

The present study demonstrates how hydrological conclusions based on geology and water levels alone can be ambiguous. For example, the water level in well ES-1 of site C is constantly about 1.5 m higher than the level in the 500 m distant wells HF- 26, 68 and 64 (Figs. 6 and 8). Hence, a flow from ES-1 in the direction of the other wells could be concluded, but the suggested 'up flow' well is significantly more saline than the 'down flow' wells (Fig. 6(b)), ruling out such a flow.

Another example of a false hydraulic gradient is provided at site T by well YT-6 which has a water level that is 3 m higher than the level in the 100 m distant well HS-41, but the salinity of the suggested 'down flow' well is significantly fresher than the 'up flow' well (Figs. 9(b) and 11).

Water flow from the area of site C to that of site T and on to site E (Fig. 1(d)) could be suggested, the water level difference being around 17 m over the short distance of 2100 m (such a gradient could indicate karstic flow!). Yet, these three sites have no hydraulic connection, based on hydrochemical evidence, supported by the geological

evidence, and confirmed by the observed high groundwater ages. Recent recharge seems to be negligible in the area studied, as indicated by the presence of shallow groundwater with an age of the order of 10 000 years, and the hydrochemically variegated nature of isolated small-scale aquifers. Under more rainy conditions the isolated water bodies would probably be interconnected by dissolution channels, lateral flow would be active, and the groundwater properties would be homogenized accordingly.

Admittedly, at the beginning of the investigation in the Be'erot area it was anticipated that the shallow wells tapped a phreatic system. Yet, the finding that these waters are old and isolated from recharge fits well with a set of new observations concerning the occurrence of isolated stagnant aquifers (groundwater traps) in other regions. For example, in the Hazeva area, in the Arava segment of the Dead Sea Rift Valley, Israel, wells at a depth of 50 m encountered pressurized water with no measurable tritium but rather high ^{14}C, allowing for a water age in the range of 50–2000 years (Fridman et al., 1993; Mazor et al., 1995, this issue). Deeper pressurized aquifers were found as well in the Hazeva region. No active recharge takes place in this area as (1) the region is very arid, and (2) the pressurized aquifers have no outcrops. Stagnant aquifers include many of the known artesian aquifers, an example being the deep inland sections of the Great Artesian Basin, Australia (Mazor, 1993; Mazor and Nativ, 1994). Thus, the Be'erot study provides an example of stagnant miniaquifers in the stage of formation.

Acknowledgments

Financial support was provided by the Ministry of Energy and Infrastructure. Support for V.F. by the J. Kassel family, Mexico, is warmly acknowledged. The Harsit Vehol Sach Co. and its geologist, Hanoch Sa'ar, are warmly thanked for the access granted to their prospecting boreholes. The chemical analyses were performed by the laboratories of the Department of Water Resources, the Desert Research Institute at Sde Boqer, and the Hydrological Service at Jerusalem. The tritium and ^{14}C measurements were conducted in the laboratory of the Department of Environmental Sciences and Energy Research, the Weizmann Institute of Science. Warm thanks are due to Dr. J. Plakht, the Ramon Science Center, Mitspe Ramon for discussions and assistance in field observations; Dr. I. Tsirlin, the Hydrological Service, Jerusalem for assistance with field observations and analytical determinations; M. Lev, the Weizmann Institute of Science, Rehovot for instrumental assistance.

References

Bartov, Y., Eyal, Y., Garfunkel, Z. and Steinintz, G., 1972. Late Cretaceous and Tertiary stratigraphy and paleogeography of southern Israel. Isr. J. Earth Sci., 21(2): 69–97.

Becker, A., 1994. Bedding-plain slip over a pre-existing fault, an example: the Ramon Fault, Israel. Tectonophysics, 230: 91–104.

Bentor, Y.K. and Vroman, A., 1951. The Geological Map of Israel 1:100 000, Avdat sheet, Israel Defense Forces, Tel Aviv, (in Hebrew).

Buchbinder, B and le Roux, J.P., 1993. Inner platform cycles in the Ardon Formation: Lower Jurassic, southern Israel. Isr. J. Earth Sci., 42: 1–16.

Fridman, V., 1994. Identifying isolated aquifers (10^2 to 10^3 meters scale), applying natural groundwater properties: examples from South Israel. M.Sc. Thesis, Weizmann Institute of Science, Rehovot.

Fridman, V., Gilad, D. and Mazor, E., 1993. Groundwater entrapment and hydraulic discontinuities within a shallow artesian system: Hazeva, Israel. Isr. Geol. Soc., Annu. Meeting, Arad, 15–18 March 1993. I. Gavrieli (Editor), Abstracts, pp. 37–38.

Garfunkel, Z., 1987. Tectonic history of Makhtesh Ramon area: general framework and problems. Isr. Geol. Soc., Annu. Meeting, Mizpe Ramon, Abstr., pp. 36–37.

Gross, M.R., 1993a. The effects of mechanical stratigraphy on failure mode and fracture spacing in the Monterey Formation of coastal California. Ph.D. Thesis, Pennsylvania State University.

Gross, M.R., 1993b. The origin and spacing of cross joints: examples from the Monterey Formation, Santa Barbara Coastline, California. J. Struct. Geol., 15: 737–751.

Hachock, P.L., 1985. Brittle microtectonics: principles and practice. J. Struct. Geol., 7: 437–457.

Hirsh, F., 1980. Jurassic bivalves and gastropods from northern Sinai and southern Israel. Israel J. Earth Sciences, 28(4): 128–163.

Hobbs, D.W., 1967 The formation of tension joints in sedimentary rocks: An explanation. Geol. Mag., 104: 550–556.

Hodgson, R.A., 1961. Regional study of jointing in Comb Ridge–Navajo Mountain area, Arizona and Utah. Bull., Am. Assoc. Pet. Geol., 45: 1–38.

Kohn, B.P., Feinstein, S. and Eyal, M., 1987. Apatite fission track dating from Ramon 1 and Hameishar 1 boreholes, reveals a Late Cretaceous cooling event. Isr. Geol. Soc., Annu. Meeting, Mizpe Ramon, 5–8 April 1987.

Kroitoru, L., Carmi, I. and Mazor, E., 1989. Groundwater ^{14}C activity as affected by initial water–rock interactions in the Judean Mountains, Israel. Chem. Geol. (Isotope Geosci. Section), 79: 259–274.

Mazor, E., 1968. Compositional similarities between hot mineral springs in the Jordan and Suez Rift Valleys. Nature, 219: 477 478.

Mazor, E., 1993. Some basic principles of ^{36}Cl hydrology — a reply to the discussion by Kellett, Evans, Allan and Fifield. Appl. Geochem., 8: 659–662.

Mazor, E. and Mero, F., 1969. The origin of the Tiberias–Noit mineral water association in the Tiberias–Dead Sea Rift Valley, Israel. J. Hydrol., 7: 334–352.

Mazor, E. and Nativ, R., 1994. Stagnant groundwaters stored in isolated aquifers: implications related to hydraulic calculations and isotopic dating — Reply. J. Hydrol., 154: 409–418.

Mazor, E., Nadler, A. and Molcho, M., 1973. Mineral springs in the Suez Rift Valley — comparison with water in the Jordan Rift Valley and postulation of a marine origin. J. Hydrol., 20: 289–309.

Mazor, E., Verhagen, B.Th., Sellschop, P.F., Jones, M.T. and Hutton, L.G., 1981. Sodium exchange in a NaCl waste disposal case (Lobatse, Botswana): implications to mineral water studies. Environ. Geol., 3: 195–199.

Mazor, E., Gilad, D. and Fridman, V., 1995. Stagnant aquifer concept Part 2. Small scale artesian systems — Hazeva, Dead Sea Rift Valley, Israel. J. Hydrol., 173: 241–261.

Zak, I., 1968. Geological Map of Israel, 1:20 000, Makhtesh Ramon, Har Gevanium. Isr. Geol. Surv., Jerusalem.